6th International Meeting
on
Wind Turbine Noise
Glasgow 20-13 April 2015

The DTU Wind Energy WTN Test Facility

Stuart Bradley Physics Department, University of Auckland, Auckland New Zealand. s.bradley@auckland.ac.nz
Torben Mikkelsen DTU Wind Energy, Roskilde, Denmark. tomi@dtu.dk
Mathew Legg Physics Department, University of Auckland, Auckland New Zealand. E-mail: m.legg@auckland.ac.nz

Summary

DTU are extending their expertise in turbine blade and aeroacoustic noise, and propagation modelling using Nord2000 and other models, by establishing a WTN Test Facility. Sites for deployment of new measurement tools include the Hϕvsϕre Test Center for Large Wind Turbines (with instrumented masts 130 m high), the Test Center at DTU Roskilde (130 m mast), and the Østerild National Test Center for Large Wind Turbines (250 m masts). Precision, fast, high-spatial resolution, wind measurements are available from DTU lidars such as WindScanner.dk.

The WTN Test Facility microphone system is based on very low noise electret microphones, calibrated against ultra-low noise GRAS 40HL microphones down to 10 Hz. The electrets are omnidirectional, and have a flat frequency response. Being inexpensive allows for a massive microphone array, capturing the WTN directionality variations, and allowing cluster configurations to reduce wind noise. Each microphone unit is autonomous and communicates to a central acquisition system, but all microphones are closely synchronized. This system design also allows for a unique Large Aperture Acoustic Camera (LAAC) to accurately pinpoint source location and characteristics in real-time, using image-sharpening algorithms developed at Auckland (the diameters of conventional commercial acoustic cameras limit their spatial resolution at WTN wavelengths).

The DTU WTN Test Facility integrates many features in a way not previously available to studies of wind turbine noise. These include the potential to set parameters of the turbine behavior (for example, yaw angle) so that controlled experiments can be conducted.

1. Introduction

DTU Wind Energy have commenced a Cross cutting activity on Wind Turbine Noise. The following includes excerpts from DTU arguments for this initiative. Public annoyance due to experienced or perceived noise from wind turbine is a significant barrier for development of wind energy on land. Wind turbine noise is a large factor of uncertainty in the planning phase of new wind farms, because state of the art noise prediction tools do not perform well or standards are not sufficient. Already installed onshore wind turbines have to run at reduced power modes, because they do not meet

the noise regulations otherwise.The public opinion about wind turbine noise and in particular low frequency noise is affected by concepts without solid scientific background and rumours. The industry has much interest in solving these problems and in clarification, quantification and standardisation in this area.

DTU Wind Energy is worldwide the only institution which has competences in wind source mapping, wind turbine aerodynamics, blade noise generation modelling and measurements, and noise propagation modelling under one roof.

The scope of wind turbine noise shall be completed by establishing a competence for outdoor noise measurements for wind turbines. In the current paper we describe initial planning for this measurement program. This will include establishing a new experimentally based noise sensing measurement facility based on a set of 48 self-sustained wireless connected sensors equipped with calibrated microphones, capable of measuring high-resolution noise time series and noise spectra including integrated noise level (dB) at deployable ranges of 0.1 to 5 km from wind farms.

In addition to broad-band noise, generally identified as trailing edge noise, there has been an increasing concern about the annoyance to people by amplitude modulation (AM) of wind turbine noise (Bowdler 2008). A study by RenewableUK (Bullmore et al. 2013) provides wide cover of different aspects of AM and the more extreme version of modulation named “other amplitude modulation” (OAM). The main hypothesis for the cause of OAM in the RenewableUK study has been that it is due to intermittent stall of a blade. Oerlemans (2013) developed a rotor simulation model including a noise model for a partially stalled airfoil and the model results showed the general observed characteristics of OAM. The source directivity characteristics of the stall noise are such that it is preferentially radiated upwind and downwind of the wind turbine and not in the cross wind direction as characterizes AM. More recently, Madsen et al. (2014) have correlated AM with turbine blade inflow conditions. They found a strong noise increase at low frequencies when a trailing edge stall initiates. For the turbine operating in a strong wind shear a modulation of the surface spectra for frequencies below 200Hz is 14dB. It was hypothesised that coupling with the turbine wake can cause abrupt changes in wind speed over the rotor disc and for a variable speed turbine the rotor might not be able to accelerate fast enough to avoid transient stall for a few revolutions. This intermittent occurrence might explain many of the occurrences of OAM.

A companion paper in WTN2015 (Bradley 2015) considers a new potential mechanism due to the time-dependent interference between sound travelling the six direct and ground-reflected paths from the three turbine blades as they rotate. One way of distinguishing between various suggested mechanisms is to use an acoustic camera. This is a synchronised array of microphones which, through appropriate phasing, can focus on the sound from discrete directions. Such a system should be able to detect intermittent stall noise since it originates at the turbine blade, but would not respond to time-dependent interference since that requires combining signals from multiple directions. Therefore, in addition to rows of autonomous and independent microphones, we plan a Large Aperture Acoustic Camera (which we abbreviate to LAAC). The reason for the large aperture, or large array diameter, is to be able to capture low frequency emissions with good angular resolution.

A substantial advantage of embedding this noise measurement project within DTU is the meteorological measurement capability of DTU, and in particular its leadership in fast short-range wind and turbulence measurements by lidar, and its excellent test sites with tall instrumented masts adjacent to test turbine stands.

2. Sites

2.1 Roskilde This site, shown in Fig. 1, is located at 55° 41' 39.20" N, 12° 5' 18.50" E and 0 m A.S.L, and is adjacent to the campus occupied by DTU Wind Energy, and so presents good opportunities for instrumentation test an development.

Figure 1. The test site at Roskilde.

In addition to comprehensive meteorological measurements at ground level, the 130 m mast has temperature measurements at 44, 117, and 122 m, wind speed at 44, 76, 92, 94, 118, and 125 m, wind direction at 76, 94, 118, and 125 m, a sonic at 122 m, and various radiation and other sensors. A number of turbines are generally under tests, some of which can be directly controlled for this project. There is about a 250 m fetch between the turbines and fjord.

2.2 Høvsøre This site (Fig. 2) is on Denmark's west coast at 56°26'47.05" N 8°09'11.10" E. Shown are 5 turbine stands accompanied by 130 m masts instrumented similarly to the Roskilde mast.

Figure 2. The test site at Høvsøre

At Høvsøre the wind conditions allow an almost uninterrupted wind speed coming from the North Sea, reaching the wind turbines at a very high speed. The flat terrain west of the test centre means that the wind conditions at the turbines are very well defined. A measuring mast is standing west of each wind turbine and a meteorology mast is situated south of the test stands. Furthermore, two 165 meters high light masts have been constructed to the east of the test stands row and they mark the maximum height of the whole area. Wind speeds, wind direction, temperatures, and atmospheric pressure are being measured on all masts, and a few of the masts provide measurements at different heights. An average wind speed of 9.3 m/s has been measured at the height of 80 meters. All data is continuously gathered.

2.3 Østerild - National Test Centre for Large Wind Turbines

Test Centre Østerild (Fig. 3) was established with 7 test stands during 2012 and allows for erection of wind turbines of up to 250 meters and accompanying mast measurements.

Figure 3. The test site at Østerild

3. Microphone array for sound propagation

An array of 48 low-noise radio-microphones are being designed for the measurement project. These are ½ inch omni-directional designs based on a very low self-noise and flat frequency response electret microphone. The design has a flat response down to about 20 Hz, and each microphone will be calibrated against several co-located GRAS 40HL low-noise microphones having measurement certificates. The GRAS microphones have a flat frequency response within ±1 dB from 12.5 Hz to 10 kHz, and within ±2 dB from 10 kHz to 16 kHz. The new electret microphones will be mounted on tripods 1.5 m above the ground.

Over the last few years considerable research has gone into the design and performance of wind shields for microphones recording low frequency noise from turbines. For example, a recent summary is given by Novak et al. (2014). Based on this summary, we have decided not to use the DELTA H secondary windscreen described in Novak et al. (2014) and elsewhere, because this configuration does not actually allow the microphone to record the sound which might be heard by a human

ear. Instead we plan to use a secondary windscreen similar to a commercial British design having a foam cylindrical structure is approximately 10 mm thick and 300 mm tall within which the microphone is centrally located.
All microphones in the measurement array will be GPS time-synchronised and will transfer data to a central computer via wireless links.

4. Large Aperture Acoustic Camera (LAAC)

A single microphone can measure the amplitude and spectrum of sound emitted by a wind turbine. However, by itself it has limited ability to determine from where on the turbine the sound is emitted. However, if the signal received from multiple microphones are processed, sound maps may be generated showing the location of sound sources (Oerlemans 2009; Simley 2010; Ramachandran et al. 2014; Oerlemans et al. 2007). These maps are often overlaid over a video camera image to form an “acoustic camera” image.

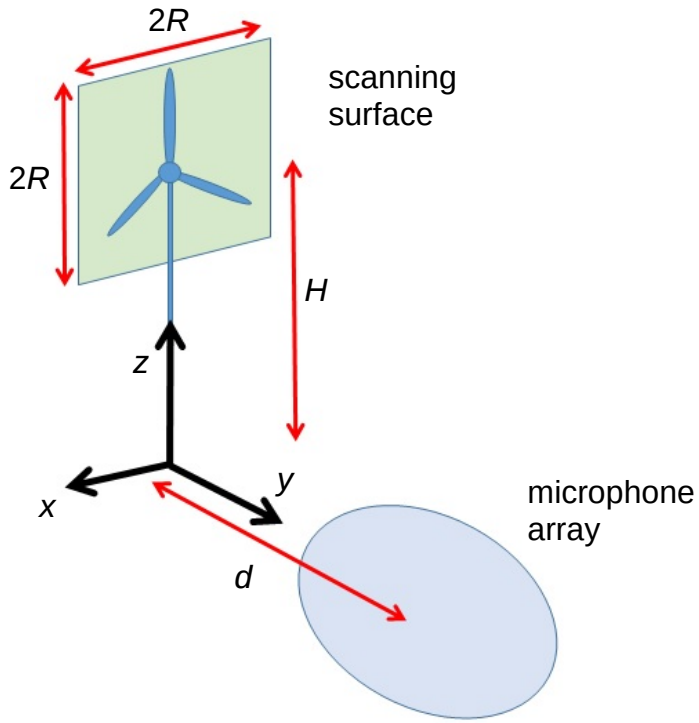

Figure 4: The coordinate system used to define the positions of the microphone array and imaging scanning surface relative to the wind turbine.

The sound emitted by the wind turbine is measured by microphones in an array which is set up some distance away (Fig. 4). A scanning surface is defined which passes through the wind turbine blades. Acoustic maps are then generated using beamforming or similar algorithms to estimate the sound source intensity at each grid point on the scanning surface. Ideally a point source would give a spike in the acoustic map corresponding to the sound source location. However, instead of a spike, beamforming produces an acoustic map which is generally composed of a main lobe and sidelobes. Figure 5 shows an example microphone array geometry and the resulting far-field beamforming beam pattern that would result from a 100 Hz point source located directly in front of the array. In order to provide the best image of the sound emitted by an object, the width of the main beam at 3 dB down from the peak, called the beamwidth, should be as small as possible while having as much intensity

separation (dynamic range) between the peak of the main beam and the peak of the largest sidelobe.

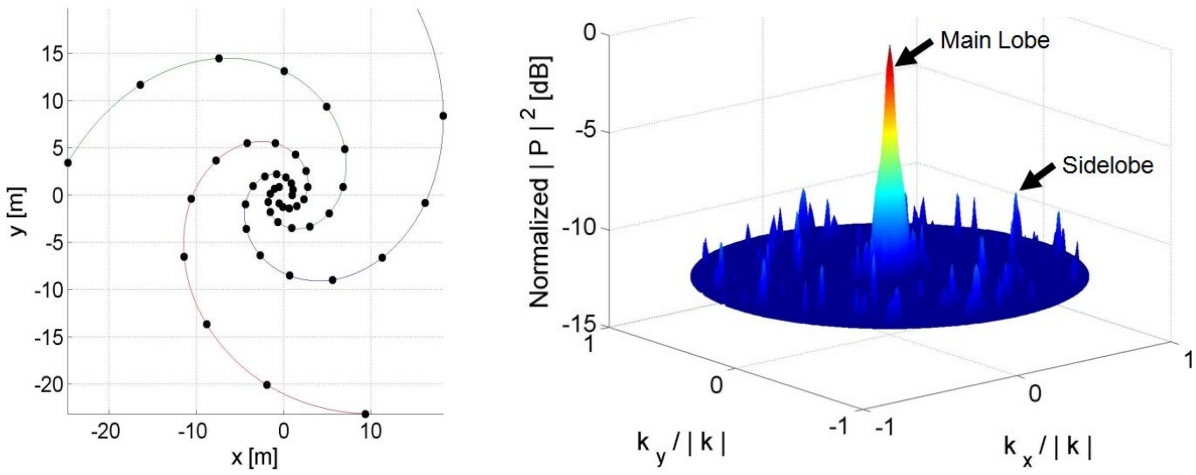

Figure 5: Microphone positions for an Underbrink multi-arm spiral array (left plot), and the far-field beam pattern for a 200 Hz point source (right plot).

The beam pattern that is achieved is dependent on the number and geometry of the microphones in the array and frequency and location of the sound source. In order to separate two sources separated by a distance *r*, the diameter *D* of the array should be

$$D \geq \frac{1.22\lambda d}{r} \tag{1}$$

where λ is the wavelength, and *d* is the distance of the sound source (Ramachandran et al. 2014). This means that the lowers the sound source frequency one wants to image, the larger the array needs to be. For example, Oerlemans et al. (2007) used a 148 element, 15 m by 18 m microphone array which provided images of sound sources down to about 630 Hz. In contrast, Ramachandran et al. (2014) used a 24 element compact array with an area of 1.5 m^2. With the use of deconvolution algorithms such as CLEAN-SC (Sijtsma 2007), TIDY (Dougherty & Podboy 2009), and DAMAS (Dougherty 2005), images were presented down to 1087 Hz which was well below that achievable using conventional beamforming.

The shape of the main lobe is dependent on the distribution of microphones in the array and the location of the sound sources. For a 2D array which has a circular distribution of microphones about the centre of the array, as in the case of the array shown in Figure 2, a symmetric main lobe may be obtained for a sound source located immediately in front of the array. However, as the sound source is moved away from the front of the array, the main lobe becomes distorted resulting in a reduced spatial resolution. In order to ensure that a symmetric beam pattern, and hence maximum spatial resolution, is achieved, elliptical shaped arrays are used for larger arrays (Oerlemans et al. 2007). Oerlemans et al. orientated the major axis towards the tip of the downwards passing blade, where the major sound sources are located. Buck et al. (2013), converted a circular Underbrink multi-arm spiral array to an elliptical shape

by multiplying the y-axis of the array by a constant. This appears to be also the method used by Oerlemans et al. (2007).

4.1 Array Hardware

We are designing a Large Aperture Acoustic Camera (LAAC) composed of a 48-element microphone array and one or more cameras. The custom built wireless microphones described in Section 3 are intended to also be used for the array. This will provide flexibility in the array design in terms of the size and layout of the array. Each microphone unit will be autonomous and communicates to a central acquisition system, but all microphones will be GPS-timing synchronized. Centrally controlled nacelle-mounted calibration sound sources will be used.

4.2 Array Shape Design

The design frequency range is 100 Hz to 5 kHz Oerlemans (2011). Ideally, in order to image sound sources with frequency content as low as 100 Hz, an array diameter of the order of 60 meters would be required. The number of microphones in our design is 48, presenting a limitation of the frequency range that would be expected to be achieved for a single array design. Therefore, at least two arrays designs will be used, a physically larger array for low frequencies and a smaller one for higher frequencies. Our array is an Underbrink multi-arm spiral array (see Figure 5) which has microphones distributed along spirals arms which are evenly spaced around a circle (Underbrink, 2002). In order to achieve good spatial resolution at low frequencies while suppressing sidelobes at higher frequencies, the array was divided into an inner and outer array part, with the inner section of the array having closer spacing of the microphones.

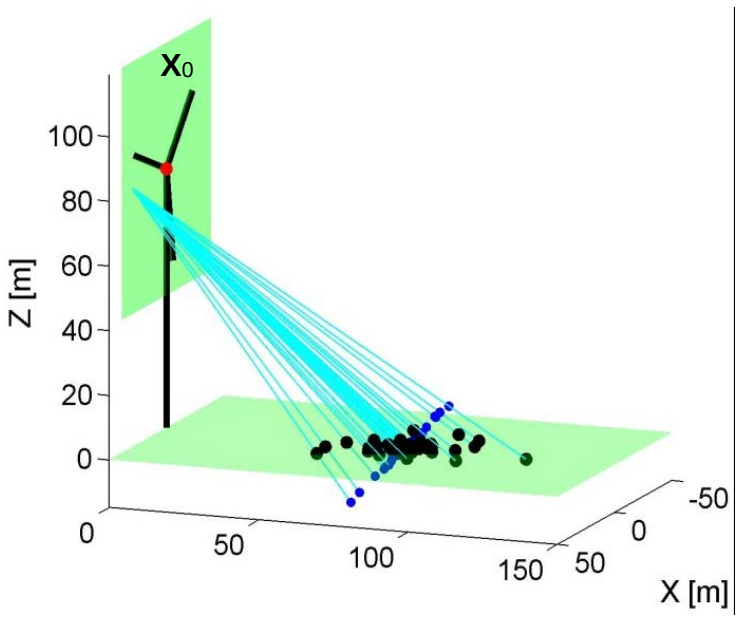

Figure 6: The projection of the microphone array coordinates shown in 4 onto the ground surface.

An Underbrink spiral array is circular in shape. However, for imaging a wind turbine using an array whose plane is horizontal, the array shape needs to be designed so that it has a circular projection onto a plane perpendicular to the turbine-array line.

Simply stretching one axis to form an elliptical array, as done by Oerlemans et al. (2007) and by Buck et al. (2013) does not allow for the wide angle subtended by the turbine at the array i.e. this does not preserve the circular array pattern when observed from a point on the rotor plane. Therefore we have a used a near-field array projection to achieve a more symmetric beam pattern.

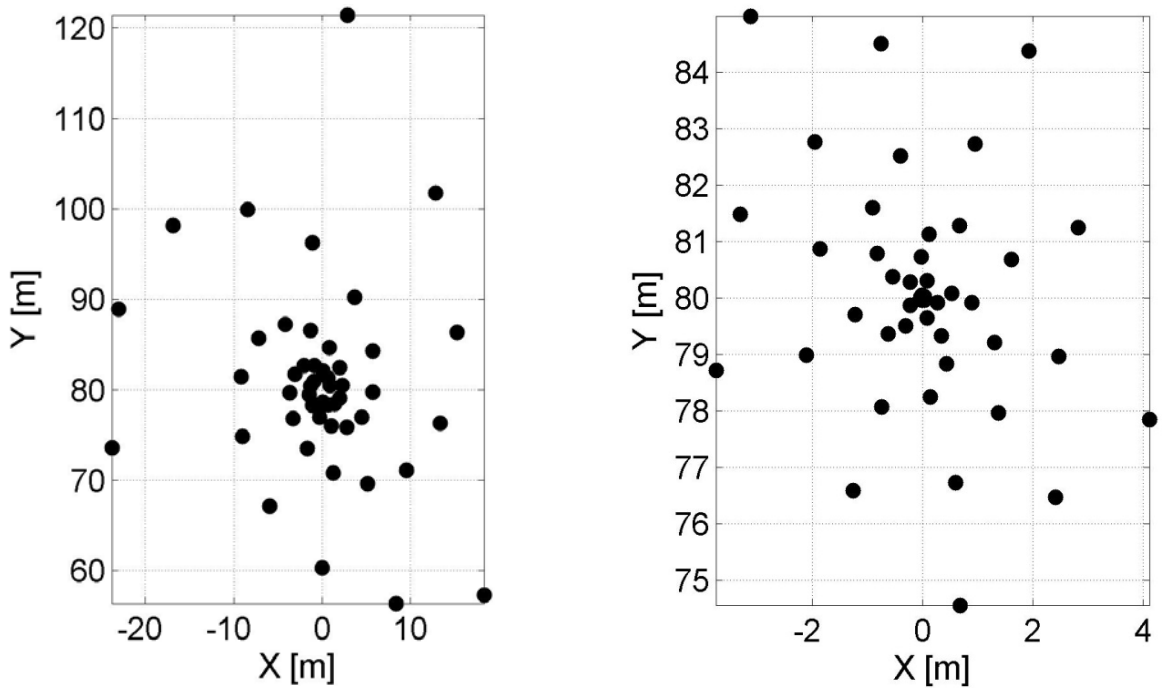

Figure 7: Microphone coordinates (after projection) of two microphone arrays. The larger of the two arrays is designed for low frequency imaging.

This conversion of the array coordinates was performed in the following manner. First a rigid body translation was used to position the circular array microphone coordinates $\mathbf{x}_j$ such that the centre of the array was a distance d from the turbine and it was orientated such that a normal to the centre of the array passed through $\mathbf{x}_0$. This was done using

$$\mathbf{x}_m = \mathbf{R}\mathbf{x}_j + \mathbf{T} \tag{2}$$

where $\mathbf{T} = [0; d; 0]$ and $\mathbf{R}$ is a rotation matrix. The matrix $\mathbf{R}$ may be calculated from the rotation vector $\boldsymbol{\alpha} = [\alpha_1; 0; \alpha_3]$, where $\alpha_1 = \pi/2\text{-}\tan^{-1}(x_3/d)$ and $\alpha_3 = \tan^{-1}(x_1/d)$. The resulting rigid body rotation and translation can be seen by the blue dots in Figure 6. These points are then projected down from the point $\mathbf{x}_0$ to the ground using

$$\mathbf{x}_p = \mathbf{x}_0 + a(\mathbf{x}_m - \mathbf{x}_0) \tag{3}$$

where a is a scalar. The projected microphone coordinates are shown as black dots in Figure 7. The resulting beam pattern is roughly elliptical but is distorted such that the microphones have a closer spacing on the side of the array towards the wind turbine.

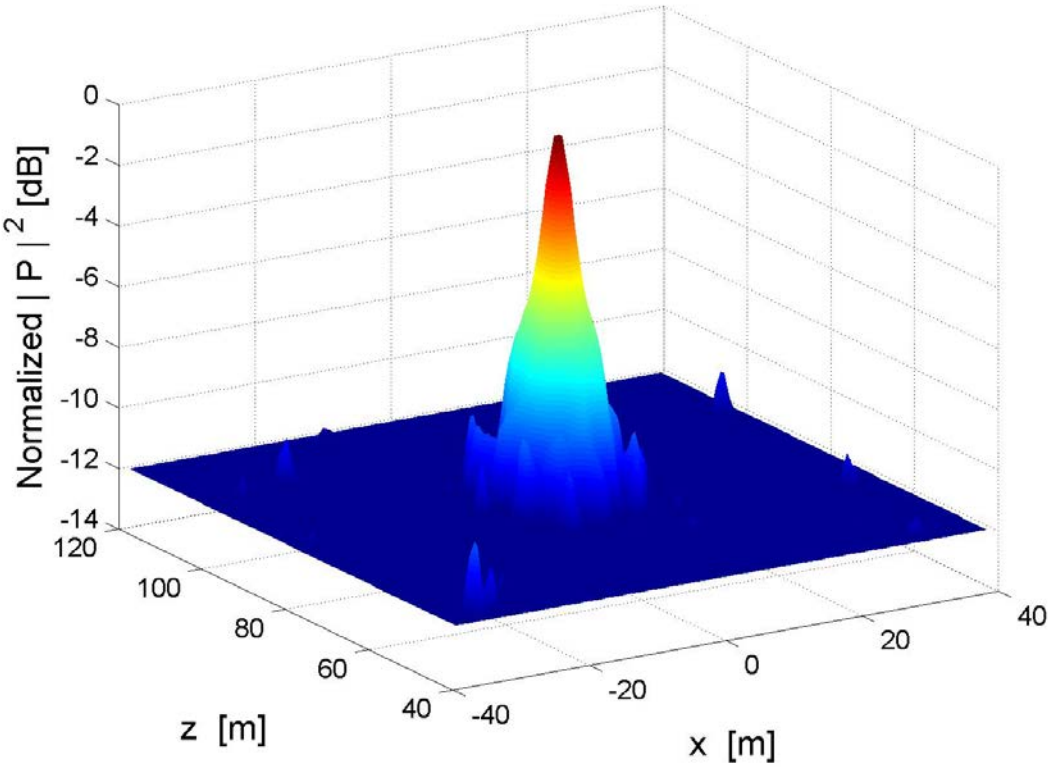

Figure 8: Normalised array point spread function for a 400 Hz point source at the hub height of 80 meters with the centre of the microphone array offset horizontally from the turbine by 100 m.

The microphone coordinates may then be used to simulate frequency domain beamforming maps (see Figure 8). This is repeated for a range of frequencies and the -3 dB beamwidth and maximum sidelobe level (MSL) are then calculated (see Figure 9). In an iterative process, this procedure is repeated for different array parameters until an optimal array design is obtained.

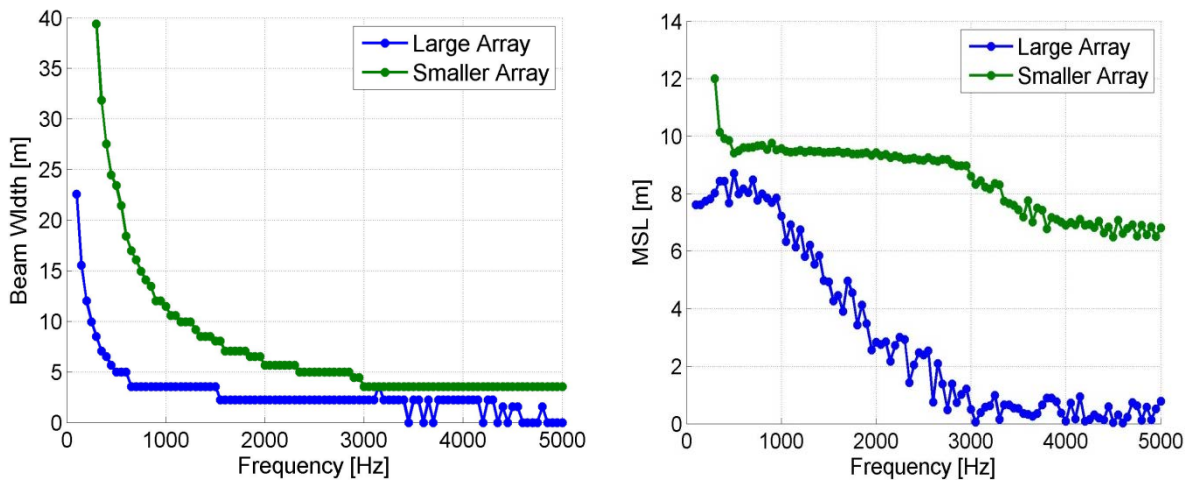

Figure 9: Plots of array beamwidth and maximum sidelobe level as a function of frequency for initials design of two low noise arrays.

4.1 Calibration

An acoustic camera is composed of an array of microphones and a video camera. In order to obtain accurate results, both the microphone array and the video camera need to be calibrated. Sound pressure level calibration of the microphones will be performed using ultra-low noise GRAS 40HL microphones which have calibration certificates down to 12.5 Hz. The microphones will be placed in their positions in the array using GPS and direct manual measurements. However, the resulting coordinates of the microphones will have some uncertainties and there may be phase variations between different channels. This can cause errors in the resulting acoustic maps meaning that microphone position calibration is likely to be needed. In addition, a video camera (or multiple cameras) will needed to be calibrated so that the acoustic maps can be accurately overlaid over the camera images. The combined calibration of the microphones and camera will be performed using sound sources at coordinates known in the camera's reference frame. See Legg & Bradley, 2013 for more details.

Another factor that is likely to cause errors in the acoustic maps is atmospheric effects. Beamforming theory assumes that the sound propagates in straight lines. However, distortion of the acoustic wave fronts due effects such as wind shear can be cause errors in the acoustic map including the location of sound sources. This effect can occur with small arrays (Bradley & Strehz 2014; Strehz 2015), but is likely to have an increased effect as the array size increases. In order to measure this effect and correct for it, calibration sound sources will be used to measure the time of flight from a number of directions at regular intervals during microphone array measurements. This will include a nacelle-mounted sound source.

4.2 Signal Processing

The signal processing will be performed using software developed at the University of Auckland. The signals measured by the array microphones will be processed to form cross spectral matrices in appropriate octave frequency bands. A scanning surface will be defined which lies in the turbine rotor plane. The scan points and the calibrated microphone coordinates will be used to generate frequency domain beamforming maps from the cross spectral matrices. Diagonal removal may be used to reduce the effect of noise such as wind noise (Dougherty 2002). Deconvolution of the beamforming maps will be performed using CLEAN-SC (Sijtsma 2007) or similar algorithms to improve the resolution and remove the effects of sidelobes. The measured time of flight from the calibration sources will be analysed and may be used to correct the acoustic maps for atmospheric effects. These resulting acoustic maps will be overlaid as transparencies over camera images. The acoustic maps will be analysed in conjunction with comprehensive meteorological measurements from mast instruments and from short range and scanning lidars.

5. Conclusions

A new comprehensive study of turbine noise is being initiated by DTU. The strengths of this program lie in DTU's ability to source in-house expertise and resources in source mapping, wind turbine aerodynamics, blade noise generation modelling and measurements, and noise propagation modelling, augmented by a growing measurement capability in outdoor noise measurements. The outdoor noise measurement part of the overall project, outlined in this paper, will be strongly supported by an existing leadership by DTU in atmospheric boundary layer measurements relevant to wind energy. In particular, DTU has excellent turbine test facilities with tall masts equipped with high quality instrumentation, and an ability to

supplement these meteorological measurements with high speed and high spatial accuracy lidar wind and turbulence measurements.
A new configurable array of radio microphones is being designed, so that any microphone can readily be placed at any location without complicated and expensive lengthy cabling. Use of GPS timing will allow for precision synchronization of the entire microphone set, including the ability to phase the array into a large aperture acoustic camera.

References

Bowdler, D., 2008: Amplitude modulation of wind turbine noise: a review of the evidence. *Institute of Acoustics Bulletin*, **33**, 31–41.

Bradley, S., 2015: Time-Dependent Interference: The Mechanism Causing Amplitude Modulation Noise? *6th International Meeting on Wind Turbine Noise Glasgow 20-13 April 2015*,.

Bullmore, A., M. Cand, S. Oerlemans, M. Smith, P. White, S. von Hünerbein, A. King, and B. Piper, 2013: *Wind Turbine Amplitude Modulation: Research to Improve Understanding as to its Cause and Effects*. RUK, http://www.renewableuk.com/en/publications/index.cfm/wind-turbine-amplitude-modulation.

Madsen, H. A., F. Bertagnolio, A. Fischer, and C. Bak, 2014: Correlation of amplitude modulation to inflow characteristics. *INTER-NOISE and NOISE-CON Congress and Conference Proceedings*, Vol. 249 of, 12136–12136.

Novak, C., A. SJÖSTRÖM, H. Ule, D. Bard, and G. SANDBERG, 2014: An investigation of Different Secondary Noise Wind Screen Designs for Wind Turbine Noise Applications. *Proc. 43rd International Congress on Noise Control Engineering (INTERNOISE 2014)*.

Oerlemans, S., 2013: An explanation for enhanced amplitude modulation of wind turbine noise. In RenewableUK 2013 report: Wind Turbine Amplitude Modulation: Research to Improve Understanding as to its Cause & Effect.

Bradley, S. & Strehz, A., 2014. Corrections to sodar Doppler winds due to wind drift. *Meteorologische Zeitschrift*.

Buck, S. et al., 2013. *Acoustic Array Development for Wind Turbine Noise Characterization*, National Renewable Energy Laboratory.

Dougherty, R.P., 2002. Beamforming in acoustic testing. In *Aeroacoustic Measurements*. Springer, pp. 62–97.

Dougherty, R.P., 2005. Extensions of DAMAS and Benefits and Limitations of Deconvolution in Beamforming. *AIAA paper*, 2961(11).

Dougherty, R.P. & Podboy, G.G., 2009. Improved phased array imaging of a model jet. In *15th AIAA/CEAS Aeroacoustics Conference (30th AIAA Aeroacoustics Conference), Miami, FL, May*. pp. 11–13.

Legg, M. & Bradley, S., 2013. A Combined Microphone and Camera Calibration Technique With Application to Acoustic Imaging. *Image Processing, IEEE Transactions on*, 22(10), pp.4028–4039.

Oerlemans, S., 2009. *Detection of aeroacoustic sound sources on aircraft and wind turbines*, University of Twente.

Oerlemans, S., 2011. *Wind turbine noise: primary noise sources*, National Aerospace Laboratory NLR.

Oerlemans, S., Sijtsma, P. & Méndez López, B., 2007. Location and quantification of noise sources on a wind turbine. *Journal of sound and vibration*, 299(4), pp.869–883.

Ramachandran, R.C. et al., 2012. Localization of wind turbine noise sources using a compact microphone array with advanced beamforming algorithms. In *4th Berlin Beamforming Conference*. pp. 22–23.

Ramachandran, R.C., Raman, G. & Dougherty, R.P., 2014. Wind turbine noise measurement using a compact microphone array with advanced deconvolution algorithms. *Journal of Sound and Vibration*, 333(14), pp.3058–3080.

Sijtsma, P., 2007. CLEAN based on spatial source coherence. *International journal of aeroacoustics*, 6(4), pp.357–374.

Simley, E.J., 2010. *Development of an Acoustic Array for Wind Turbine Aeroacoustic Noise Analysis*. Citeseer.

Strehz, A., 2015. *Development of a Bi-static Addition for MINI-SODARs*. Auckland, New Zealand: Department of Physics, University of Auckland.

Underbrink, J.R., 2002. Aeroacoustic phased array testing in low speed wind tunnels. In *Aeroacoustic measurements*. Springer, pp. 98–217.